Spring 5-9-2020

Determining the Kinetic Isotope Effect of Ruthenium Compound $Ru(bpy)_2(bpyNO)(PF_6)_2$ Using Artificial Photosynthesis

Alexandra I. Kirkvold
University of South Dakota

Determining the Kinetic Isotope Effect of Ruthenium Compound $Ru(bpy)_2(bpyNO)(PF_6)_2$ Using Artificial Photosynthesis

by

Alexandra Kirkvold

A Thesis Submitted in Partial Fulfillment
Of the Requirements for the
University Honors Program

Department of Physics
The University of South Dakota
May 2020

The members of the Honors Thesis Committee appointed
to examine the thesis of Alexandra Kirkvold
find it satisfactory and recommend that it be accepted.

_____

Dr. Dongming Mei
Professor of Physics
Director of the Committee

_____

Dr. Wenqin Xu
Assistant Professor of Physics

_____

Dr. Tina Keller
Professor of Physics

ABSTRACT

Determining the Kinetic Isotope Effect of Ruthenium Compound $Ru(bpy)_2(bpyNO)(PF_6)_2$ Using Artificial Photosynthesis

Alexandra Kirkvold

Director: Dr. Dongming Mei

The world's demand for energy is ever-increasing, but its fuel resources are being depleted at an alarming rate. A potential solution for this crisis lies in using ruthenium-based compounds to produce hydrogen for use in fuel cells. This research uses the process of artificial photosynthesis to learn more about a promising ruthenium-based compound, $Ru(bpy)_2(bpyNO)(PF_6)_2$. The experiment tests the reaction for oxygen production in both H_2O and D_2O to determine the Kinetic Isotope Effect of the compound and, thus, aid future research working to understand the reaction mechanisms. The analysis shows that the reaction demonstrates an inverse Kinetic Isotope Effect. However, the study was limited by the consistency of the equipment's measurements and the small number of tests that were able to be completed. Further work with this compound should address this issue and aim to produce more conclusive results than the ones obtained by this study. However, this experiment provides knowledge to the scientific field that is pioneering research of clean, alternative fuel using artificial photosynthesis.

Key Words: Kinetic Isotope Effect; Artificial photosynthesis; Oxygen production; Ruthenium; Water splitting

TABLE OF CONTENTS

LIST OF FIGURES

ACKNOWLEDGEMENTS

I would like to give a special thanks…

To the REU program at Purdue University, especially my supervisor Dr. Yulia Pushkar: for giving me the opportunity to complete this research and for providing me with invaluable skills and knowledge both for research and life. Thank you for teaching me.

To Dr. Tina Keller: for welcoming me into the physics department at USD and for always helping me in my pursuits, both professional and personal. You have inspired me with your strength as a woman in STEM and opened my eyes to my full potential. Thank you for being the one to give me my first position in the lab; without you, none of this would have been possible.

To Dr. Dongming Mei: for providing me with amazing opportunities that I never thought I would have access to. Because of you, I have traveled across the country and the world. The opportunities that you have provided taught me so much about scientific research, other cultures, and myself. Thank you for allowing me to work with you for four years and for believing in me, even when I didn't believe in myself.

To Dr. Wenqin Xu: for opening my eyes to the impact of research and for being so willing to help me when I needed it. You were a great teacher, both as a professor and as a life mentor. I cannot thank you enough for your kindness and the knowledge you have given me.

To my friends and family: Clara, Ashleigh, Emily, Madi, Kyler, and many others, thank you for standing by me unconditionally. I would not be the person I am today without you; you all have changed me and my life for the better. I love you. Thank you.

CHAPTER 1. INTRODUCTION

In this chapter, we look at the big picture motivating this experiment, especially concerning the energy crisis that our generation is facing. This experiment aims to add to the knowledge and understanding of possible solutions for the issues surrounding fuel sources. Additionally, this chapter provides the basic background knowledge needed to understand the mechanics of the experiment.

1.1 MOTIVATION

As the human population has grown, so has our demand for energy. From 1980 to 2017, there was a 94% increase in energy consumption worldwide and the Global Energy Outlook projects it to increase another 34% by the year 2050 (Newell et al., 2019). This demand has been met by a variety of energy sources with certain advantages and disadvantages. Some of the energy sources, such as hydroelectric, wind, and solar, are classified as renewable energy sources, meaning that the source cannot be depleted or can be renewed within a human lifetime (Frewin, 2020). However, only about 20% of the energy consumed worldwide is derived from renewable resources. The vast majority, around 80%, of the world's energy is sourced from fossil fuels, such as coal, natural gas, and oil (International Energy Association, 2020). These fossil fuels are a nonrenewable resource and extracting them from the Earth both generates pollution and harms local ecosystems. Furthermore, when these fuels are produced, transported, and burned, they emit harmful greenhouse gases, such as carbon dioxide, methane, and nitrous oxide, which contribute to climate change and global warming (United States Environmental Protection Agency, 2019a).

The basics of global warming are quite simple to understand. When sunlight reaches the Earth, the energy is either reflected back into space or absorbed and re-radiated as heat. This process is natural and relatively harmless unless there is a significant presence of greenhouse gases in the atmosphere. Greenhouse gases absorb most of the energy that would otherwise be reflected into space, and scatters it all directions, warming the Earth in the process (NASA, 2020). The higher the concentration of greenhouse gases in the atmosphere, the more warming occurs.

The evidence of rapid climate change is overwhelming. The average surface temperature on Earth has increased 1.62 degrees Fahrenheit since the late 19th century and the average ocean surface temperature (top 700 meters) has increased 0.4 Fahrenheit since 1969. All over the world snow and ice extent and thickness has declined, with the rate of ice mass loss in Antarctica tripling over the last decade. This has all resulted in a global sea level rise of around 8 inches in the last century, with the past two decades doubling in rate (NASA, 2019). The Intergovernmental Panel on Climate Change has estimated that there is more than a 95% possibility that the warming our planet has experienced over the past 50 years is directly caused by human activities.

In order to combat the effects of global warming, an alternative to nonrenewable energy must be found. Governments all over the world are already implementing solar, wind, and hydroelectric energy sources as alternatives to unrenewable methods of providing electricity to homes and businesses. However, this does not address the harmful effects that traditional combustion engine vehicles have on the environment. Transportation accounts for 29% of greenhouse gas emissions in the United States, making it the largest single contributor to greenhouse gas emissions (United States Environmental

Protection Agency, 2019b). Strides have been made in the electric car industry, however these alternatives still use fossil fuels indirectly, as most electricity in the United States is sourced from fossil fuels and contributes greatly to overall greenhouse gas emissions. Ideally, an alternative fuel source for cars that would not need to rely on the established electrical grid, instead it would be able to function similarly to traditional gas-powered cars without contributing any harmful effects to the environment. One particularly promising alternative is hydrogen.

Hydrogen is the lightest, and therefore most abundant element in the universe. When harnessed and used as fuel, it can be burned with oxygen to produce clean energy in the reaction:

$$2H_2(g) + O_2\ (g) \rightarrow H_2O\ (g) + energy$$

Furthermore, the technology already exists to take advantage of this reaction. Hydrogen fuel cells can be used in cars as a clean alternative to combustion engines. As shown in the equation, in an ideal atmosphere of pure oxygen, the only byproducts of this reaction are energy and water vapor. If carried out in atmospheric air, the reaction may also yield small amounts of nitrogen oxides, a common type of greenhouse gas. However, hydrogen fuel cells produce 97% less nitrogen oxides than conventional coal-fired powerplants (U.S. Fuel Cell Council, 2010). Hydrogen is therefore much cleaner than traditional fuels that generate harmful gases like methane and carbon dioxide, in addition to nitrogen oxides, when used. Not only are hydrogen fuel cells less impactful to the environment, they also have two to three times more fuel efficiency than tradition combustion engines (US Department of Energy, 2020). Moreover, unlike other alternatively fueled vehicles, cars with hydrogen fuel cells have similar fueling procedures to traditional cars, making the conversion from

gas-powered cars to fuel cell cars even easier. In fact, several states, such as California, already use fuel cell buses and have hydrogen fueling stations.

With all the promise that hydrogen shows as an alternative fuel source, one can only wonder why it is not more widely used. As previously mentioned, hydrogen is the most abundant element in the universe, however it is rarely found in its pure form. Most hydrogen is produced by steam reforming natural gas, commonly by extracting it from methane. This method, however, releases greenhouse gases like carbon dioxide and carbon monoxide into the atmosphere (Liu et al., 2010). Another production method of hydrogen is electrolysis, where an electric current is run through water to separate the oxygen atoms from the hydrogen. However, this method can also be carbon intensive if it uses electricity generated from nonrenewable sources. Additionally, the electricity used could be used instead for existing electric car technologies, rather than creating the hydrogen for fuel cells. Because it requires so much energy to split water molecules into hydrogen and oxygen, hydrogen fuel technology has been overlooked by other promising forms of renewable fuel. However, for billions of years, plants and other organisms have been using the process of photosynthesis to efficiently harness and store energy by splitting water into its components.

1.2 PHOTOSYNTHESIS

Photosynthesis is the conversion of solar energy, carbon dioxide, and water into fuel with the general reaction:

$$6CO_2 + 6H_2O + photons \rightarrow C_6H_{12}O_6 + 6O_2$$

Modern plant cells capture light using photosystem proteins, which are complex systems of molecules like chlorophylls and carotenoids. These molecules absorb and use light to energize electrons, which are then harnessed to power the plant cell. If we are able to understand this process, then we could use an artificial form of photosynthesis to split water molecules and produce clean hydrogen to be used as fuel elsewhere.

During the process of photosynthesis, Photosystem II (PSII), a photoactive metalloprotein complex found in plant cells, splits water molecules into oxygen, protons, and electrons through water oxidation. In PSII, the process begins when a photon is absorbed by the chlorophyll and one of its electrons is promoted to a higher energy. This electron is then passed down to the other parts of the reaction center: plastoquinone A and plastoquinone B. Once enough energy has accumulated, the small quinone is released from the photosystem and is delivered to the next step in the electron transfer chain. Because this leaves the original chlorophyll without an electron, it takes one from a water molecule (Protein Data Bank, 2004). The oxygen-evolving center in PSII uses the Mn_4O_5Ca cluster to remove four electrons from two water molecules, creating oxygen gas (O_2) and four hydrogen ions ($4H^+$).

The key to this process is the Mn_4O_5Ca cluster, which triggers the water splitting reaction:

$$2H_2O + photons \rightarrow 4H^+ + 4e^- + O_2$$

Because the Mn_4O_5Ca cluster is the catalyst, it could potentially be used in artificial photosynthesis. Unfortunately, many studies have found that it does not last long enough in man-made setups to be used effectively. It is unstable, insoluble in water, and requires intricate systems like the ones found in plants in order to function properly. Therefore, the

search continues for a compound that can be successfully used in a lab setting to most proficiently perform artificial photosynthesis. Ruthenium compounds have yielded promising results, and so they were the primary focus of my lab. I experimented with several different ruthenium complexes to find which performed artificial photosynthesis the most efficiently. My primary focus, however, was on the compound $Ru(bpy)_2(bpyNO)(PF_6)_2$.

$Ru(bpy)_2(bpyNO)(PF_6)_2$ was the most promising compound, as it had demonstrated that it could produce large amounts of oxygen reliably, which meant that it was splitting water into its parts efficiently. The difficult part of hydrogen production is not harnessing the hydrogen from the reaction, it is completing the process of splitting water. I was asked, then, to learn more about this compound and how we could most ideally structure its reaction to yield the most desirable results possible. The best way to do this was to determine the Kinetic Isotope Effect.

1.3 Kinetic Isotope Effect

The Kinetic Isotope Effect (KIE) is considered to be one of the most essential tools used for the study of reaction mechanisms. It is a phenomenon where replacing one of the atoms in the reactants with one of its isotopes causes the reaction rate to change (Libretexts, 2020). The KIE is a ratio between the rate constants of a chemical reaction where a light element (k_L) is replaced by its heavier isotope (k_H).

$$KIE = \frac{k_L}{k_H}$$

A common isotope substitution, and one that we used in our experiment, is replacing hydrogen with deuterium. For the lighter complex, we used

$Ru(bpy)_2(bpyNO)(PF_6)_2$ with water (H_2O) as the solute and for the heavier complex we used $Ru(bpy)_2(bpyNO)(PF_6)_2$ with heavy water (D_2O) as the solute to determine the KIE of the reaction. Typically, substituting heavier isotopes leads to a slower reaction rate, so a normal KIE has a value greater than one, while an inverse KIE has a value less than one. It was extremely important to determine the KIE, as we were using a complex that has not been extensively studied in the existing literature. Furthermore, understanding the reaction mechanisms would allow us to take full advantage of the dynamics of the reaction and produce the most oxygen possible.

CHAPTER 2. EXPERIMENT

In this chapter, I explain the necessary equipment required to complete the experiment testing the compound $Ru(bpy)_2(bpyNO)(PF_6)_2$. Furthermore, I go into detail on the specifics of the procedure used, as it is extremely important in understanding how the results were obtained.

2.1 EQUIPMENT AND MATERIALS

In order to test the ruthenium compounds, we first have to make them. During the course of the experiment, I ran tests on several different ruthenium complexes all with slightly different preparation processes. However, the main focus of this paper is the $Ru(bpy)_2(bpyNO)(PF_6)_2$ compound, so it is the only one I will explain in explicit detail. Most of the other compounds, though, have similar enough preparation procedures that this section could be used as a guide for preparing them, too. Perhaps the only difference in preparation is in regards to the light sensitivity of $Ru(bpy)_2(bpyNO)(PF_6)_2$. Any exposure to light could compromise the integrity of its performance, so any preparations and tests done with $Ru(bpy)_2(bpyNO)(PF_6)_2$ were completed in darkness. In order to see, I used a low intensity, red headlamp because it would not affect the compound as severely as bright, white, overhead lights would.

$Ru(bpy)_2(bpyNO)(PF_6)_2$ came in the form of a powder solvent so that I could decide what molarity to mix it to. After calculating and measuring the mass of powder needed, I would add in the exact amount of liquid, typically either H_2O or D_2O, needed with air displacement micropipettes. These are adjustable micropipettes that use piston-driven air

displacement to pick up an extremely precise volume of liquid. They use disposable tips, so the source liquid will not get contaminated when picking up a volume. Because many of the powders had low solubility in water, I often added a small amount of 1 mM trifluoroethanol (TFE) as a solvent. I also used a vortex mixer to ensure that the solutions were completely mixed. Once the compounds were made, I moved on to testing them.

The most important piece of equipment for the experiment is the Oxygraph (Figure 1). I used the Hansatech Oxygraph+ System, which is optimized for liquid test samples.

Figure 1. The Hansatech Oxygraph+ system. (Hansatech, n.d.).

The Oxygraph uses a Clark type electrode in order to measure the concentration of oxygen in the liquid. The device consists of an epoxy resin disk (Figure 2) that is placed beneath the testing chamber, with a platinum cathode and silver anode set into it. The electrode is isolated from the testing chamber by an oxygen-permeable Polytetrafluoroethylene (PTFE) membrane, so that the platinum is protected and any fouling or metal plating is reduced. A paper spacer soaked with a 50% saturated KCl solution is placed between the membrane and electrodes to provide a uniform layer of electrolyte between the anode and the cathode. Together the membrane and paper are held close to the surface of the cathode with a small O-ring. A larger O-ring is placed into a

circular well surrounding the electrodes to prevent any of the liquid sample from leaking. Then, a small voltage is applied across the electrodes. The platinum electrode acts a cathode, so it has a negative charge and the silver anode a positive one. The oxygen permeates the membrane and is reduced at the cathode. During reduction, the oxygen acts as an acceptor and acquires an electron, meaning that the process requires a steady current of electrons dependent on the rate at which the oxygen can reach the electrode. Therefore, the current that flows is directly related to amount of oxygen that is consumed at the cathode. The higher the current, the higher the concentration of oxygen in the liquid being tested.

Figure 3. The epoxy resin disk complete with the center cathode and ring anode. The O-rings are placed for demonstration, but the required PTFE membrane and paper spacer are omitted. (Hansatech, n.d.)

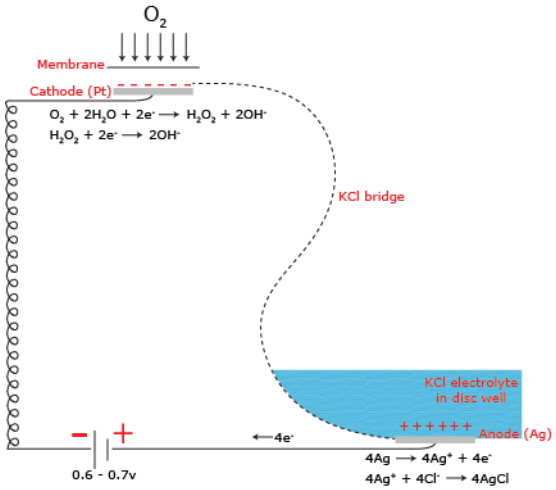

Figure 2. A cross section of the electrode demonstrating the flow of current and the anatomy of the system. (Hansatech, n.d.)

Hansatech provides a software called OxyTrace+ to be used for data acquisition and hardware control. To start taking data, I simply plugged the Oxygraph+ system into a computer's USB port. The software displays the data being taken in real time and can be used for post-acquisition data analysis like the calculation of oxygen rates. However, I transferred the data from OxyTrace+ to Microsoft Excel for analysis and compilation. I found that it was much easier to directly compare two different runs through Excel than through the OxyTrace+ software, and I was more comfortable running calculations in Excel because I have used the software for years.

2.2 PROCEDURE

To start the experiment, I first made the $Ru(bpy)_2(bpyNO)(PF_6)_2$ compound that needed to be tested. Because I was focused on determining the KIE of the compound I made two separate mixtures of $Ru(bpy)_2(bpyNO)(PF_6)_2$, one in H_2O and one in D_2O. I began by determining the molar mass of the compound so that I could calculate the amount to be mixed into the correct molarity needed. In the case of $Ru(bpy)_2(bpyNO)(PF_6)_2$, I found the molar mass to be 593g/mol.

Because the experiment was completed over the course of two months, I attempted to reduce any degradation of the compound by only making the amount of compound necessary for the next few tests. This means that I made several batches of $Ru(bpy)_2(bpyNO)(PF_6)_2$ over the course of the experiment and I did not use the exact same measurements every time. However, to aid with clarity, I will go through the process of making one specific batch of compound. In this instance, I had 4.8 mg total of the compound. Because I needed to make two solutions, I divided it roughly in half. It ended up that 2.3 mg of $Ru(bpy)_2(bpyNO)(PF_6)_2$ went into the H_2O solution and 2.5 mg into the

D_2O solution. The final desired molarity of both solutions was 1 mM, so I needed 2.3 mL and 2.5 mL of solution, respectively. I added 200 μL of TFE to each solution to aid with dissolving the solute, filled the rest in with either H_2O or D_2O, and mixed with the Vortex mixer. So, finally, I ended up with two different 1 mM solutions: one consisting of 2.3 mg of $Ru(bpy)_2(bpyNO)(PF_6)_2$, 2.1 mL of H_2O, and 200 μL TFE and one consisting of 2.5 mg $Ru(bpy)_2(bpyNO)(PF_6)_2$, 2.3 mL D_2O, and 200 μL TFE.

Once the solutions were mixed and ready to be tested, it was time to calibrate the Oxygraph. The Oxygraph does not have an absolute scaling system, so every time I ran any tests I needed to calibrate it. This would ensure that I could convert my measurements into usable values. To calibrate, I first needed to take measurements of a liquid with a known value of oxygen concentration at normal atmospheric pressure and temperature. Water has an oxygen concentration of about 272.26 μmol/L, so I used that to calibrate.

First, I filled the chamber with pure, deionized water and let it run for about 30 seconds to establish a baseline. Then, I added sodium dithionite to react with the oxygen and thus decrease the concentration to 0 μmol/L. Sodium dithionite, or sodium hydrosulfite has a reaction in water of:

$$Na_2S_2O_4 + O_2 + H_2O \rightarrow NaHSO_4 + NaHSO_3$$

Once I add a large amount of sodium dithionite to the water in the oxygraph, all of the oxygen reacts away, leaving an actual concentration of 0 μmol/L. However, as seen on the graph of a calibration run shown below, the values measured by the oxygraph are not the same as the actual values. Instead of displaying a range in concentration from 273.26 μmol/L to 0 μmol/L, we see that the measurements ranged from around 1500 to 30. Because

of this disparity, I used the method of linear mapping to convert the measurements to usable data, which I further explain in Chapter 3.1.

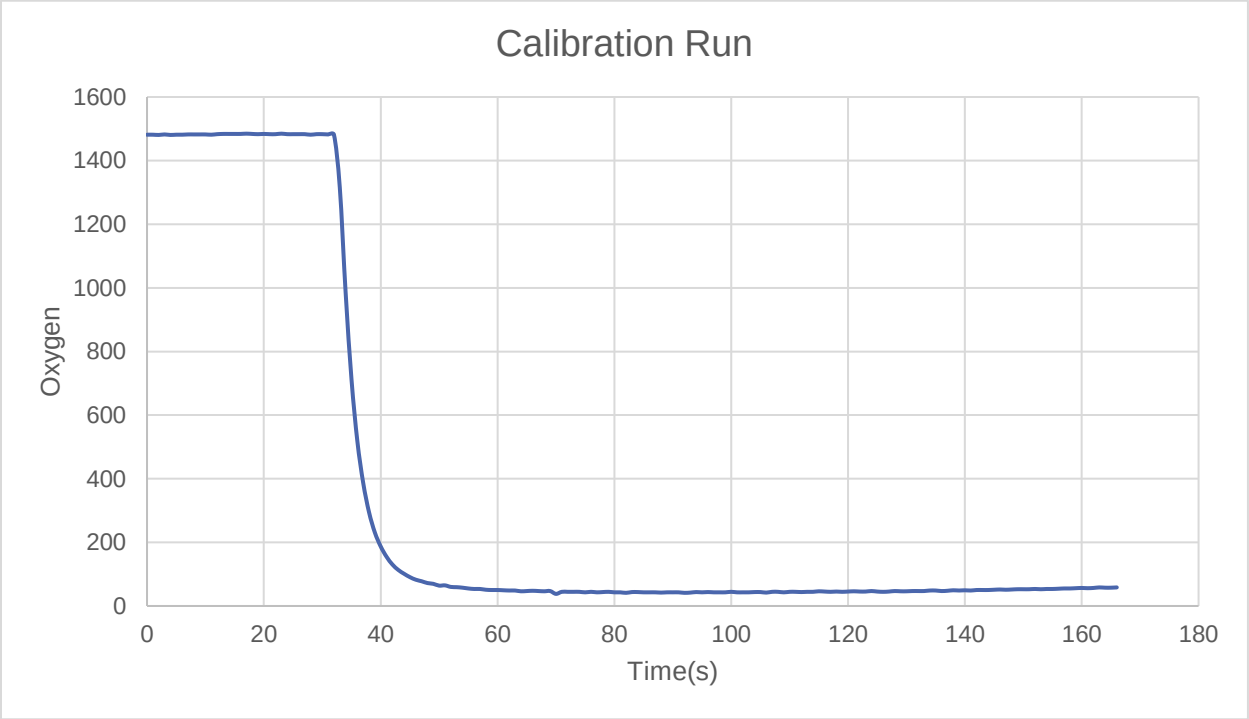

Figure 4. A typical calibration run of the Oxygraph, demonstrating the reaction between deionized water and sodium dithionite.

To aid with accuracy, I then rinsed out the oxygraph with deionized water and ran two more calibration runs. This allowed me to take an average of the three calibrations and get a more accurate result.

Once the Oxygraph was calibrated, I could begin my tests on the $Ru(bpy)_2(bpyNO)(PF_6)_2$ compounds. The first step of testing the compounds was to change the pH to 1. We used 1 M Cerium (IV) Ammonium Nitrate (CAN) as a catalyst, which required that the solution have a pH of 1 to work. The definition of pH is:

$$pH = p[H^+] = -\log_{10} a_{H^+}$$

Where $[H+]$ is the concentration of hydrogen ions in the solution and a_{H^+} is the hydrogen ion activity of the solution. HNO_3 has a hydrogen ion activity level such that its a_{H^+} is

simply the molarity of the solution. To change the pH, I used 1 M HNO_3 which, when calculated with the above equation, has a pH of 0. To change the $Ru(bpy)_2(bpyNO)(PF_6)_2$ compound's pH to 1 then, we simply need to solve for a_{H^+} in the equation.

$$1 = -\log_{10} a_{H^+}$$

so,

$$a_{H^+} = 0.1M$$

This means that we need to fill the chamber with a solution of 1 part HNO_3 and 9 parts $Ru(bpy)_2(bpyNO)(PF_6)_2$. Therefore, I filled the chamber with 100 μL of HNO_3 and 900 μL of $Ru(bpy)_2(bpyNO)(PF_6)_2$ either the H_2O or D_2O solution. After doing so, I then waited 60 seconds before adding the CAN catalyst.

CAN is a one-electron oxidizing agent that is commonly used to catalyze oxidative addition reactions (Organic Chemistry Portal, n.d.). In the experiment, it was used to catalyze the reaction between the $Ru(bpy)_2(bpyNO)(PF_6)_2$ compounds and the electrode of the Oxygraph. I added between 10 and 40 equivalents of CAN, most often 20 equivalents. Because the CAN had a concentration of 1 M, while the $Ru(bpy)_2(bpyNO)(PF_6)_2$ compounds usually had one of 1 mM, 20 equivalents was a relatively small amount. The total volume of 1 mM $Ru(bpy)_2(bpyNO)(PF_6)_2$ solution was only 1 mL, so for 20 equivalents of 1 M CAN I only needed to add 20 μL.

Once all of this preparation was complete, the reaction would begin, and oxygen would start being produced. Then, like before, the Oxygraph would begin measuring the total oxygen concentration. The graph would show an increase in oxygen concentration as more O_2 would be produced, and I could use this data to determine the KIE of the compound.

CHAPTER 3. RESULTS

In this chapter, I look into the data and results to determine the KIE of $Ru(bpy)_2(bpyNO)(PF_6)_2$. The process of converting the measurements using the calibration is also thoroughly explained and used to analyze the results.

3.1 DATA

Once I finished my tests, I started to work with the data to determine the KIE of $Ru(bpy)_2(bpyNO)(PF_6)_2$. As mentioned before, the raw data from the Oxygraph is not usable because it is unitless, meaning that it is on a completely different scale and cannot be used in any sort of comparison. However, the calibration measurements taken at the beginning of every testing session could be used to solve this issue. Because the calibration measurements started with a known value of oxygen concentration in water at standard conditions, 272.26 μmol/L, and ended with total depletion of the oxygen, 0 μmol/L, the simple method of linear mapping could be used to understand the oxygraph's scale.

The concept of linear mapping is easy to understand, as it uses the standard equation of a line, $y = mx + b$, and can be explained using a simple graph. To demonstrate, I will use some actual raw data acquired from the Oxygraph during one of the tests for $Ru(bpy)_2(bpyNO)(PF_6)_2$. To find the linear mapping equation, I only need the minimum and maximum values of oxygen concentration found by the oxygraph, then I can apply the equation to the rest of the raw data to get usable results in the correct units of concentration, μmol/L.

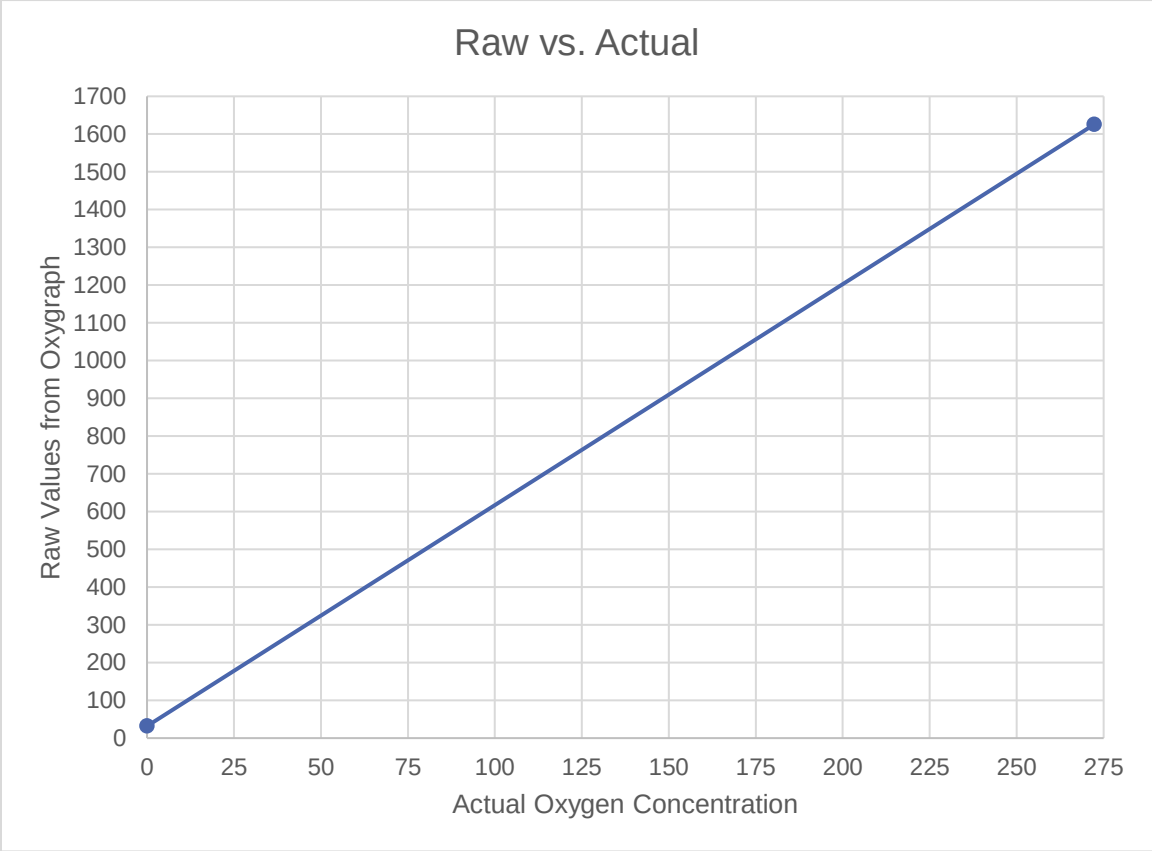

Figure 5. A demonstration of the disparity between the values measured by the Oxygraph and the actual values of oxygen concentration. Notice the difference between the zero points of the two scales.

On the x-axis we have the actual oxygen concentration. Because of the water used during the calibration portion, the values range from 0 μmol/L (no oxygen) to 272.26 μmol/L (the concentration of oxygen in water at standard conditions). The y-axis shows the raw values that the oxygraph output during the calibration. We know that the minimum value of raw data corresponds to 0 μmol/L and the maximum value corresponds to 272.26 μmol/L, so we draw a line connecting those two points. The slope of this line is simply the difference between the maximum and minimum of the raw data over the difference between the maximum and minimum of the actual values, or, more concisely,

$\frac{\max(raw)-\min(raw)}{\max(ac)-\min(ac)}$. We know that the y-intercept is simply the minimum of the raw data, so we can plug these values into the line equation, $y = mx + b$, where x is the actual value of the oxygen concentration and y is the raw data from the oxygraph:

$$n_{raw} = \frac{\max(raw) - \min(raw)}{\max(ac) - \min(ac)} * n_{ac} + \min(raw)$$

So, to convert our raw data into the actual values of oxygen concentration, we simply solve for n_{ac}, getting:

$$n_{ac} = (n_{raw} - \min(raw)) * \frac{(\max(ac) - \min(ac))}{(\max(raw) - \min(raw))}$$

Applying this to the raw measurements yields useable, meaningful data that we can then analyze.

3.2 Analysis

Once I converted the unitless measurements into meaningful data using the calibration runs, I could start determining the rates of oxygen production. First, I plotted the calibrated data on a graph so it would be easier to visualize and understand the different parts of the curve. Shown below is one of the runs using $Ru(bpy)_2(bpyNO)(PF_6)_2$ in D_2O.

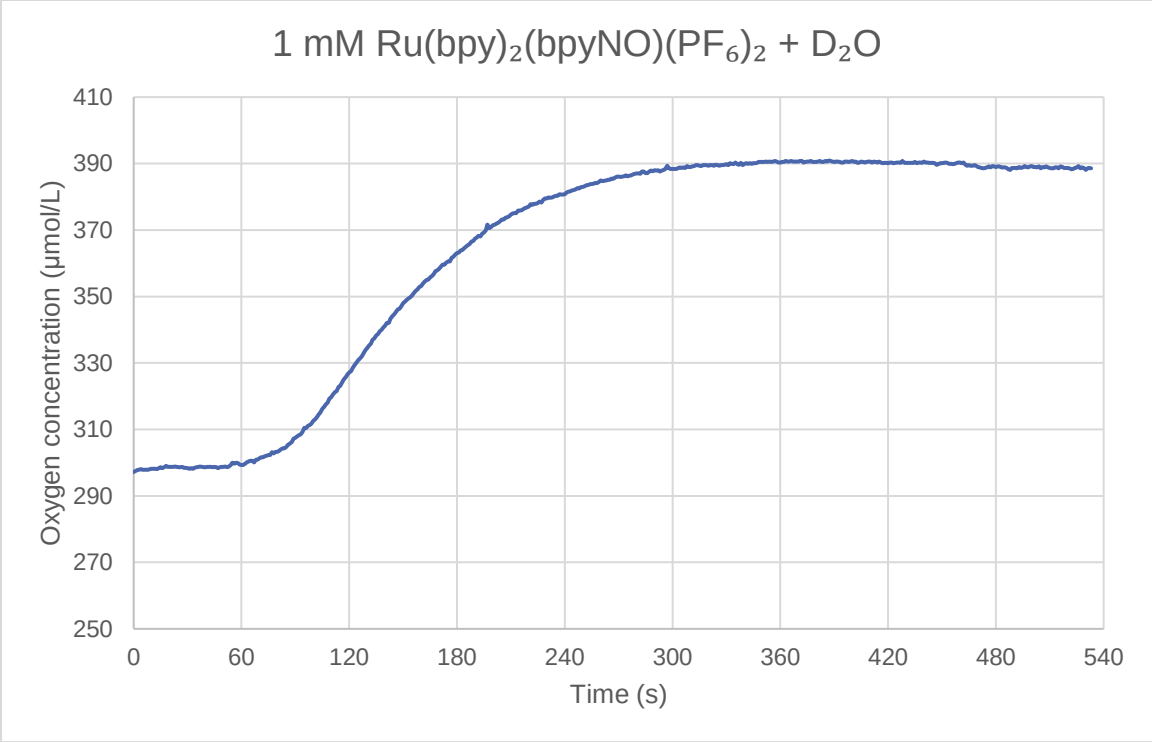

Figure 6. A successful test of $Ru(bpy)_2(bpyNO)(PF_6)_2$ in D_2O showing how the oxygen concentration changes over time as it is being produced by the reaction.

During the first 60 seconds, the curve is flat because I had not added the CAN yet, so there was no oxygen being produced. After adding the catalyst, oxygen concentration began to increase until the solution was completely oxidized and could no longer be reduced at the cathode. Therefore, no more oxygen was produced, and the reaction was complete.

The goal of the experiment is to compare the rates of the compound's oxygen production in H_2O and D_2O to find the KIE. The rate of oxygen production is simply the slope of the graph because it shows how the oxygen concentration changes over time. To compare, I took the slope at the same point for the compound in both H_2O and D_2O. I tried to take the slope when the graph was the straightest and showed the largest increase in oxygen production to ensure that the differences were noticeable and accurate. Therefore,

I compared the highest rate of each compound by taking the slope at the steepest point of oxygen production. For the above plot of $Ru(bpy)_2(bpyNO)(PF_6)_2$ in D_2O, I used the rate from 90s to 180s and found it to be 0.618 μmol/L·s. To find the KIE, we need the rates from $Ru(bpy)_2(bpyNO)(PF_6)_2$ in both H_2O and D_2O, so below is the next run completed with H_2O as the solute.

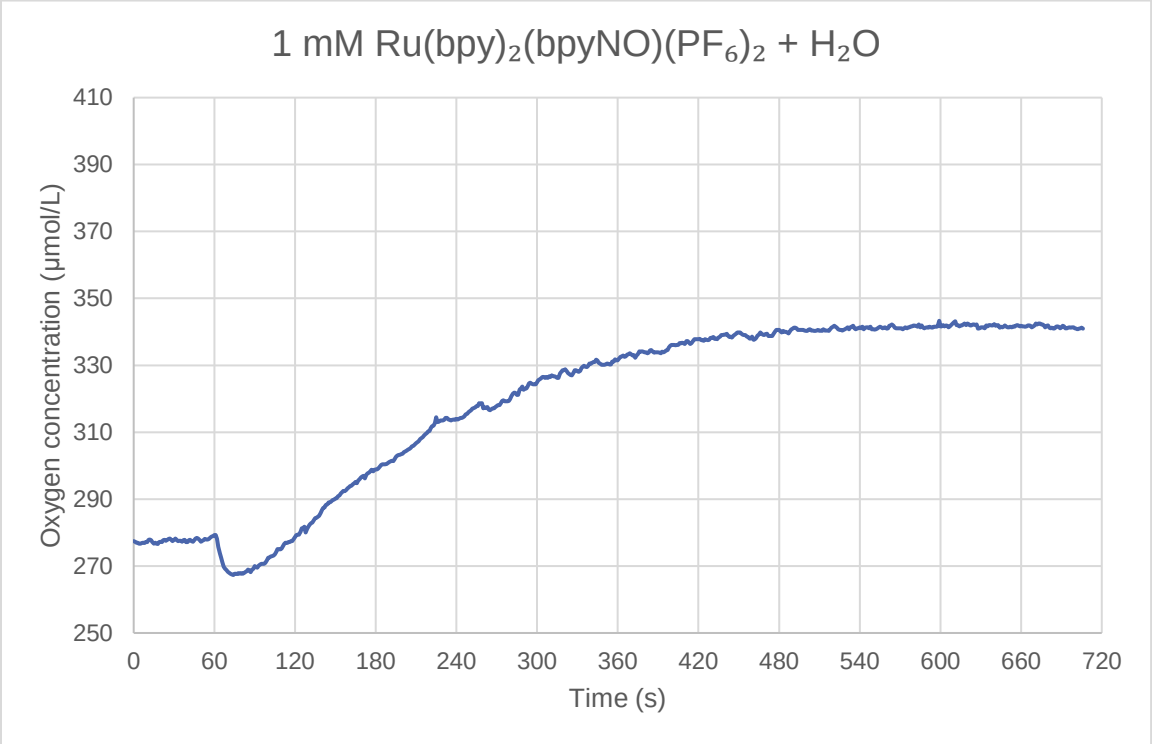

Figure 7. A successful test of $Ru(bpy)_2(bpyNO)(PF_6)_2$ in H_2O showing how the oxygen concentration changes over time as it is being produced by the reaction.

For this run, I found the rate from 90s to 180s to be 0.321 μmol/L·s, meaning that it had a lower rate of production than the compound in D_2O. For the results to be as accurate as possible, though, I took the average rates of oxygen production found from several different runs of $Ru(bpy)_2(bpyNO)(PF_6)_2$ dissolved in either H_2O or D_2O and compared the two to find the KIE.

Using the definition of the KIE, $KIE = \frac{k_L}{k_H}$, where k_L is the rate of the compound's oxygen production in H_2O and k_H is the rate in D_2O, we find $KIE = \frac{0.254}{0.737} < 1$. This means that the reaction demonstrates an inverse KIE.

Concentration (mM)	**Solvent**	**CAN equivalents**	**Rate (µmol/L·s)**	**Standard Deviation**
1	H_2O	20	0.254	0.192
1	D_2O	20	0.737	0.511

CHAPTER 4. DISCUSSION

After finding that the reaction involving the compound $Ru(bpy)_2(bpyNO)(PF_6)_2$ demonstrates an inverse KIE, I discuss the implications of the result. Additionally, I explore the limiting factors of the experiment and my recommendations for further research.

4.1 INTERPRETATIONS AND IMPLICATIONS

The rates of oxygen production indicate that the reaction involving the compound $Ru(bpy)_2(bpyNO)(PF_6)_2$ demonstrates an inverse KIE, meaning it has a higher reaction rate in heavy water, D_2O, than it does in pure water, H_2O. You might notice that this means the hydrogen in the reaction is replaced with deuterium. For those unfamiliar with deuterium this may seem like a confusing exchange, because the motivation for the experiment was to find a reaction that could split water and yield usable hydrogen molecules. To address this issue there are several answers. First, deuterium is simply a heavier isotope of hydrogen, being exactly the same but with one neutron added to its atom. This means that it is comparable to hydrogen and the reaction could potentially still be fruitful for hydrogen production. Second, learning about the reaction, even if it does not produce perfect results, is always helpful for adding knowledge to the ever-growing information base. Therefore, this result does not mean that the reaction cannot be used to harness hydrogen from water, it only means that we can begin to understand the reaction mechanisms determining the rate. The KIE is one of the most essential tools for studying reaction mechanisms. Understanding the reaction mechanism allows us to increase the efficiency of reactions by

improving the desirable qualities. Determining the KIE does not tell us everything about the reaction, but it is the first step to more fully understanding it. More research needs to be done in order to idealize the reaction.

4.2 Limitations and Future Research

There were a few limitations that could potentially be improved upon in further tests. For one, the oxygraph does not produce completely consistent results. This was something that the lab team I worked with stressed to me from day one. The standard deviation of the results emphasizes this, as it is nearly the same as the average rates. In order to prove consistent results and achieve the ideal precision, the standard deviation should be much smaller than the average rates. One way to improve this would be to increase the number of trials so that hopefully the standard deviation would decrease. However, this would not address the actual problem. Finding the sources of error in the oxygraph would be more useful in increasing the precision of the results. I investigated certain parameters, such as cleanliness of the cathode and anode, but was unable to produce any conclusive results. Further experimentation with the experiment conditions could yield some interesting realizations that may improve the consistency of the measurements.

Furthermore, improvement of the data analysis techniques could aid in reducing error and increasing the precision of the results, potentially lowering the standard deviation. For example, fitting the results to a logistic function and obtaining the parameters for carrying capacity and maximum rate could be used to both calibrate the Oxygraph and produce better results for the rate. The logistic function is a S-shaped curve, very similar

in appearance to the graphs of oxygen production found in the experiment. The function is defined as

$$f(x) = \frac{L}{1 + e^{-k(x-x_0)}}$$

Where x_0 is the value of the sigmoid's midpoint, L is the curve's maximum value, and k is the logistic growth rate or the steepness of the curve. The standard logistic function (where L = 1, k = 1, and x_o = 0) is shown below.

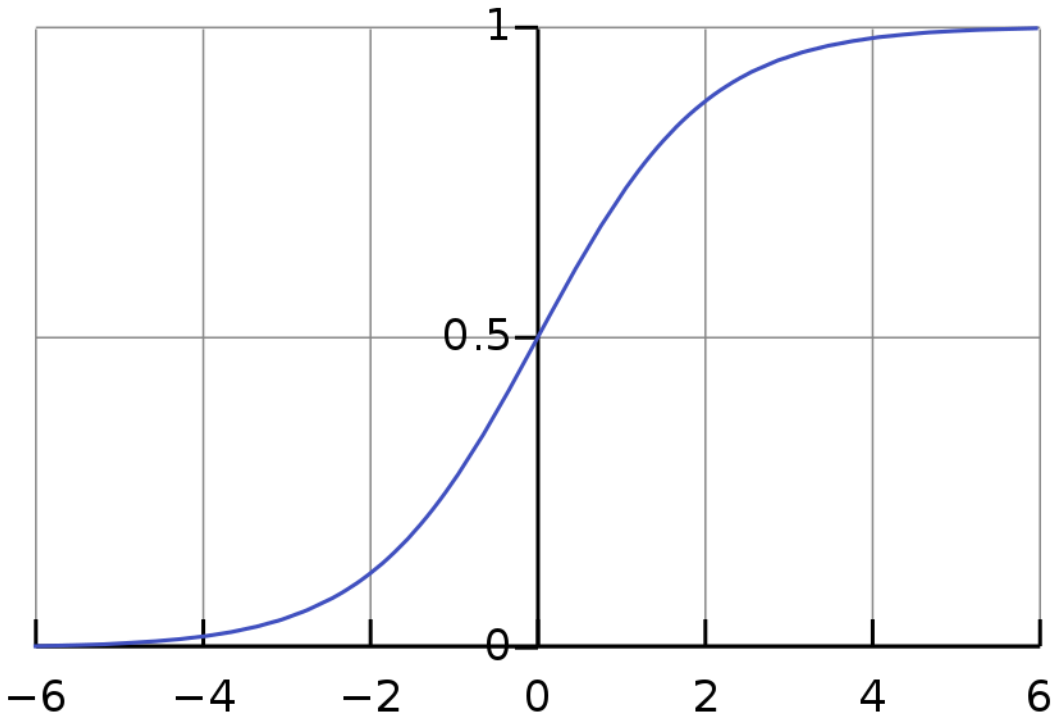

Figure 8. The standard logistic sigmoid function, where L = 1, k = 1, x_0 = 0.

The logistic function has several mathematical properties that could be used to analyze the data found and provide a more robust explanation of the measurements.

CHAPTER 5. CONCLUSION

This research aimed to determine the KIE of the compound $Ru(bpy)_2(bpyNO)(PF_6)_2$ to add to the research being conducted on artificial photosynthesis. The rate of the reaction was measured by finding the rate of oxygen production when the compound was both in H_2O and D_2O. Because the rate of the reaction was higher with the heavier isotope, the reaction was found to have an inverse Kinetic Isotope effect. Further research is needed to determine the reaction mechanisms and to apply this research to the search for clean fuel alternatives.

When I first started this experiment, not much was known about the compound. This research provides knowledge for any future experimentation, as the KIE of the reaction was completely unknown. Determining the KIE is a necessary step to deciding whether further research could provide a solution to the problem of splitting water to harness hydrogen. My findings add to the literature of the scientific field studying artificial photosynthesis.

Though my experiment has concluded, there is still a lot to learn about using ruthenium-based compounds for artificial photosynthesis. There is a long road of research ahead, but the results could have an astounding impact. If artificial photosynthesis is utilized to effectively and efficiently produce hydrogen, then the future of clean fuel would be changed forever. It is very possible that the day will come where ruthenium-based compounds are used to power our homes and cars, hopefully solving much of the environmental crisis we are currently facing.

CHAPTER 6. REFERENCES

Frewin, C. (2020, May). Renewable Energy. Retrieved from https://www.studentenergy.org/topics/renewable-energy

Hansatech. (n.d.). Oxygraph System. Retrieved from http://www.hansatech-instruments.com/product/oxygraph-system/

International Energy Association. (2020, May 1). Energy Data and Statistics. Retrieved from https://www.iea.org/data-and-statistics/data-tables?country=WORLD

Libretexts. (2020, May 18). Kinetic Isotope Effects. Retrieved from https://chem.libretexts.org/Bookshelves/Physical_and_Theoretical_Chemistry_Textbook_Maps/Supplemental_Modules_(Physical_and_Theoretical_Chemistry)/Quantum_Mechanics/06._One_Dimensional_Harmonic_Oscillator/Kinetic_Isotope_Effects

Liu, K., Song, C., & Subramani, V. (2010). *Hydrogen and Syngas Production and Purification Technologies*. Hoboken, NJ: Wiley. doi: 10.1002/9780470561256

NASA. (2019). Climate Change Evidence: How Do We Know? Retrieved from https://climate.nasa.gov/evidence/

NASA. (2020). The Causes of Climate Change. Retrieved from https://climate.nasa.gov/causes/

Newell, R. G., Raimi, D., & Aldana, G. (2019). *Global Energy Outlook 2019: The Next Generation of Energy*. Resources for the Future.

Organic Chemistry Portal. (n.d.). Cerium Ammonium Nitrate, CAN. Retrieved from https://www.organic-chemistry.org/chemicals/oxidations/ceriumammoniumnitrate-can.shtm

Protein Data Bank. (2004). Photosystem II. Retrieved from http://pdb101.rcsb.org/motm/59

U.S. Fuel Cell Council. (2010). *U.S. Fuel Cell Council Industry Overview 2010* (p. 12).

United States Environmental Protection Agency. (2019). Overview of Greenhouse Gases. Retrieved from https://www.epa.gov/ghgemissions/overview-greenhouse-gases

United States Environmental Protection Agency. (2019, April). Sources of Greenhouse Gas Emissions. Retrieved from http://www.epa.gov/ghgemissions/sources-greenhouse-gas-emissions

US Department of Energy. (2020, March 11). Compare Fuel Cell Vehicles. Retrieved from https://www.fueleconomy.gov/feg/fcv_sbs.shtml